DALTON

exo,*endo* and *exo*,*exo* isomers of 6,9-$(PMe_2Ph)_2$-*arachno*-$B_{10}H_{12}$ and its halogenated derivatives. Molecular structures of *exo*,*endo*- and *exo*,*exo*-6,9-$(PMe_2Ph)_2$-*arachno*-$B_{10}H_{12}$ and *exo*-6,*endo*-9-$(PMe_2Ph)_2$-2-Br-*arachno*-$B_{10}H_{11}$

Udo Dörfler, Thomas D. McGrath, Paul A. Cooke, John D. Kennedy and Mark Thornton-Pett

The School of Chemistry of the University of Leeds, Leeds, UK LS2 9JT

Reaction of PMe_2Ph with *nido*-$B_{10}H_{14}$ at *ca.* 200 K gave *exo*,*exo* and *exo*,*endo* isomers of 6,9-$(PMe_2Ph)_2$-*arachno*-$B_{10}H_{12}$ which were separated chromatographically. Both forms were confirmed crystallographically. The compounds 2-Br-*nido*-$B_{10}H_{13}$ and 2,4-Cl_2-*nido*-$B_{10}H_{12}$ gave exclusively *exo*,*endo* forms at *ca.* 200 K with the 2-Br product consisting of equal amounts of 6-*endo*-9-*exo* and 6-*exo*-9-*endo*-$(PMe_2Ph)_2$ isomers, demonstrating no directional control by the 2-Br substituent. The relative configurations of the two brominated isomers were confirmed by a crystallographic study of the 6-*exo*-9-*endo* species. Both the monobrominated *exo*,*endo* isomers gave the *exo*,*exo* counterpart on heating, but the 2,4-Cl_2 species is more robust, with apparent decomposition on extended heating, and no evidence for the formation of *exo*,*exo*-6,9-$(PMe_2Ph)_2$-2,4-$Cl_2B_{10}H_{10}$.

Since the discovery in 1957 that *nido*-decaborane, $B_{10}H_{14}$, readily reacts with nucleophilic bases L to give *arachno* species 6,9-$L_2B_{10}H_{12}$ **1** [equation (1)][1] the reaction has become very well

$$B_{10}H_{14} + 2L \longrightarrow \underset{\mathbf{1}}{L_2B_{10}H_{12}} + H_2 \qquad (1)$$

recognized,[2] not least because of the importance of these species (where L is a weaker base) as intermediates in *closo* twelve-vertex dicarbaborane formation.[3] The original crystallographically characterized examples of these $L_2B_{10}H_{12}$ species **1** were for L = MeCN and SMe_2, and these exhibited an *exo*,*exo* bis(ligand) disposition **IA**.[4,5] This configuration is also shown by more recent crystallographic studies,[6,7] and it seems reasonable to presume that this is the most stable thermodynamic configuration. However, in 1987 it was reported[8] that NMR spectroscopy showed that careful addition of the ligand PMe_2Ph to *nido*-$B_{10}H_{14}$ at lower temperatures gave substantial quantities of the *exo*,*endo* 6,9 isomer **1b** of configuration **IB** as well as the expected *exo*,*exo* isomer **1a**. This was not associated with any crystallographic work. The *exo*,*endo* isomer **1b** isomerized to the *exo*,*exo* 6,9 isomer **1a** of configuration **IA** on mild heating. More recently it was reported that, where L = pyridine (py), a third type of isomer can be formed, the *exo*,*endo* 6,6 isomer of configuration **IC**.[9] This also has not yet been substantiated crystallographically, the only $(py)_2B_{10}H_{12}$ isomer so investigated being the conventional *exo*,*exo* 6,9 isomer of configuration **IA**.[7] We have now investigated our PMe_2Ph system in more detail, with the intention of crystallographic confirmation of the *exo*,*endo* 6,9 isomeric form **IB**, and, with a view to the examination for any *exo*/*endo* directional control or other isomer preferences, using the halogenated *nido*-decaboranes 2-$BrB_{10}H_{13}$ and 2,4-$Cl_2B_{10}H_{12}$ as starting substances. We now report results from these investigations. The numbering system used for the *nido* and *arachno* ten-vertex geometry is in schematic **II**.

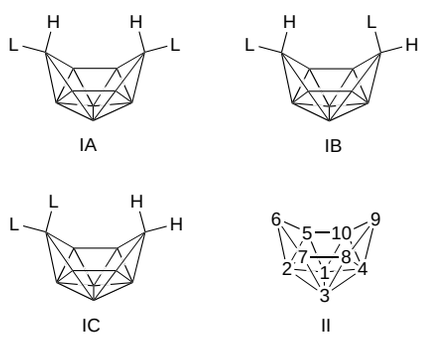

Results and Discussion

It has previously been reported that the addition of PMe_2Ph to $B_{10}H_{14}$ at low temperature, followed by warming to room temperature, results in a *ca.* 60%:40% mixture of the *exo*,*exo* and *exo*,*endo* isomers of 6,9-$(PMe_2Ph)_2$-*arachno*-$B_{10}H_{12}$[8] **1a** and **1b** respectively. At the time the formation of the *exo*,*endo* isomeric forms of this type of *arachno* species 6,9-$L_2B_{10}H_{12}$ had not previously been noted. The *exo*,*endo* isomer **1b** was readily identified in this first instance by NMR spectroscopy on the *exo*,*exo*/*exo*,*endo* mixture of compounds **1a** and **1b**.[8] We have now found in this work that chromatography on silica gel G using hexane–CH_2Cl_2 (1:9) as solvent can result in the isolation of the two isomers in pure form, isolatable in yields of 57 and 34% respectively. Crystallization from CH_2Cl_2–hexane at room temperature gave single crystals of each that were suitable for X-ray diffraction analysis. The crystallographically determined molecular structure of the *exo*,*exo* isomer **1a** (Fig. 1 and Tables 1 and 2)[10] confirms this isomer to have the two phosphine ligands in *exo*,*exo* dispositions (schematic **IA**), whereas the structure of **1b** (Fig. 2 and Tables 1 and 2) clearly confirms its formulation as the *exo*,*endo*-6,9-$(PMe_2Ph)_2$-*arachno*-$B_{10}H_{12}$ isomer (schematic **IB**) and obviously precludes, for example, the 6,6-*exo*,*endo* configuration **IC**.

For the *exo*,*exo* isomer **1a** there are two crystallographically independent molecules (designated A and B) in the asymmetric fraction of the unit cell. The borane clusters of these two molecules are essentially identical within experimental error; they differ in the conformations of the organic moieties bound to phosphorus. Most significant are the twists of the phosphorus-bound phenyl rings about the P–C (Ph) vectors. The ring bound to P(1) in molecule B is twisted by 66.8(4)° relative to that in A, whilst that bound to P(2) in B is twisted by 88.0(4)° relative to that in A. The two molecules of compound **1a** and that of **1b** all have the classical *arachno* ten-vertex character typical of such 6,9-bis(ligand)decaborane species, and in particular have

Table 1 Selected interatomic distances (Å) and angles (°) for the two crystallographically independent molecules (A and B) of *exo*,*exo*-6,9-$(PMe_2Ph)_2$-*arachno*-$B_{10}H_{12}$ **1a**, *exo*,*endo*-6,9-$(PMe_2Ph)_2$-*arachno*-$B_{10}H_{12}$ **1b** and, for comparison, the two crystallographically independent molecules (X and Y)[11] of [*endo*,*endo*-6,9-μ-PPh_2-*arachno*-$B_{10}H_{12}$]$^-$ **2** (schematic **III**)

	1a (A)	**1a** (B)	**1b**	**2** (X)	**2** (Y)
B(2)–B(5)	1.751(4)	1.754(4)	1.765(2)	1.72(2)	1.75(2)
B(2)–B(6)	1.744(5)	1.740(4)	1.735(2)	1.75(2)	1.77(2)
B(2)–B(7)	1.758(5)	1.752(4)	1.758(2)	1.72(2)	1.71(2)
B(5)–B(6)	1.865(5)	1.867(4)	1.851(2)	1.90(2)	1.96(2)
B(6)–B(7)	1.860(4)	1.877(4)	1.864(2)	1.89(2)	1.86(2)
B(6)–P(1)	1.912(3)	1.925(3)	1.9145(14)	1.888(13)	1.918(13)
B(4)–B(8)	1.748(5)	1.760(4)	1.758(2)	1.71(2)	1.74(2)
B(4)–B(9)	1.748(4)	1.732(4)	1.762(2)	1.74(2)	1.78(2)
B(4)–B(10)	1.766(4)	1.755(5)	1.756(2)	1.75(2)	1.75(2)
B(8)–B(9)	1.876(4)	1.859(4)	1.888(2)	1.89(2)	1.88(2)
B(9)–B(10)	1.873(4)	1.866(4)	1.883(2)	1.84(2)	1.87(2)
B(9)–P(2)	1.925(3)	1.914(3)	1.941(2)	1.890(14)	1.884(12)
B(5)–B(10)	1.869(4)	1.879(4)	1.892(2)	1.89(2)	1.86(2)
B(7)–B(8)	1.875(5)	1.871(4)	1.879(2)	1.90(2)	1.90(2)
B(2)–B(6)–P(1)	110.6(2)	107.0(2)	111.20(8)	112.6(8)	124.5(8)
B(5)–B(6)–P(1)	119.3(2)	117.3(2)	118.23(8)	95.5(6)	95.4(7)
B(7)–B(6)–P(1)	118.6(2)	116.5(2)	120.18(8)	95.0(7)	96.6(7)
B(4)–B(9)–P(2)	105.8(2)	111.1(2)	155.86(10)	124.1(9)	125.4(8)
B(8)–B(9)–P(2)	116.4(2)	117.1(2)	111.33(8)	95.8(8)	96.3(7)
B(10)–B(9)–P(2)	116.8(2)	120.3(2)	110.42(8)	95.4(7)	96.7(7)
B(6)–B(5)–B(10)	113.2(2)	113.5(2)	112.88(9)	105.9(9)	105.5(9)
B(5)–B(6)–B(7)	103.8(2)	104.1(2)	104.52(9)	105.1(8)	103.5(8)
B(6)–B(7)–B(8)	113.1(2)	112.3(2)	113.22(9)	107.4(9)	107.3(8)
B(7)–B(8)–B(9)	113.2(2)	113.4(2)	115.96(9)	106.3(9)	106.0(8)
B(8)–B(9)–B(10)	103.7(2)	104.8(2)	101.91(9)	107.1(9)	106.5(8)
B(9)–B(10)–B(5)	113.3(2)	111.9(2)	116.10(9)	108.3(9)	108.3(8)
B(1)–B(2)–B(6)	115.4(2)	116.4(2)	115.21(10)	114.9(9)	113.8(8)
B(3)–B(2)–B(6)	115.7(2)	116.5(2)	115.74(10)	114.4(9)	112.4(8)
B(1)–B(4)–B(9)	116.3(2)	115.6(2)	118.32(10)	114.2(10)	113.9(8)
B(3)–B(4)–B(9)	116.9(2)	115.9(2)	118.38(10)	113.2(10)	113.0(8)

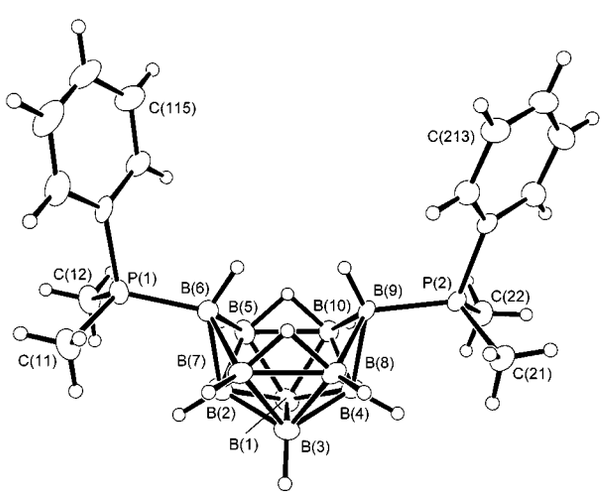

Fig. 1 An ORTEP-type[10] drawing of the crystallographically determined molecular structure of one of the crystallographically independent molecules (A) of *exo*,*exo*-6,9-$(PMe_2Ph)_2$-*arachno*-$B_{10}H_{12}$ **1a** with thermal ellipsoids shown at the 40% probability level. Phenyl rings C(*n*1*i*) (*n* = 1 or 2, *i* = 1–6) are numbered cyclically and hydrogen atoms have been assigned a small, arbitrary radius for clarity. Molecule B only differs significantly from A in the orientation of the phosphorus-bound substituents

B(5)–B(10) and B(7)–B(8) connectivities [range 1.869(4)–1.892(2) Å] characteristically shorter than the corresponding distance (typically *ca.* 2.00 Å) in *nido*-decaboranyl clusters. The presence of a hydrogen atom bridging each of these vectors is further consistent with their *arachno* constitution.

The effect upon structure of an *exo versus* an *endo* phosphine substituent may be evaluated by comparison of the selected geometric parameters given in Table 1, in which salient distances and angles for compounds **1a** (A and B) and **1b** are listed. Also included for comparison are the corresponding values for what formally constitutes an *endo*,*endo* analogue, the [*endo*,*endo*-6,9-μ-(PPh_2)-*arachno*-$B_{10}H_{12}$]$^-$ anion **2** of schematic structure **III** (which has two crystallographically independent molecules X and Y in its crystallographically examined $[PMePh_3]^+$ salt).[11] Unfortunately the reported structure of this *endo*,*endo* species **2** is insufficiently accurate for a detailed comparison with the present compounds. It does appear, however, that the boron–phosphorus distances B(6)–P(*endo*) and B(9)–P(*endo*) in compound **2** [1.884(12) to 1.918(13) Å] tend to be rather shorter than those in **1a** and **1b**. This might equally be a consequence of stereochemical constraints arising from the bridge, or of the differing chemical nature of this anion.

Table 2 Additional interatomic distances (Å) and angles (°) for the two crystallographically independent molecules (A and B) of *exo*,*exo*-6,9-$(PMe_2Ph)_2$-*arachno*-$B_{10}H_{12}$ **1a** and *exo*,*endo*-6,9-$(PMe_2Ph)_2$-*arachno*-$B_{10}H_{12}$ **1b**

	1a (molecule A)	**1a** (molecule B)	**1b**
B(1)–B(2)	1.769(5)	1.762(4)	1.769(2)
B(1)–B(3)	1.812(5)	1.819(5)	1.816(2)
B(1)–B(4)	1.765(5)	1.769(5)	1.755(2)
B(1)–B(5)	1.766(5)	1.781(5)	1.779(2)
B(1)–B(10)	1.788(4)	1.778(5)	1.791(2)
B(2)–B(3)	1.766(5)	1.769(5)	1.765(2)
B(3)–B(4)	1.767(4)	1.767(5)	1.754(2)
B(3)–B(7)	1.783(5)	1.781(4)	1.774(2)
B(3)–B(8)	1.788(5)	1.783(5)	1.789(2)

Cluster B–B–B acute angles are within the ranges: **1a** (A) 57.3(2)–64.9(2), **1a** (B) 57.0(2)–65.0(2) and **1b** 57.15(7)–64.88(8)°.

Table 3 Measured ^{11}B and ^{1}H NMR chemical shift data for *exo*,*exo*-6,9-$(PMe_2Ph)_2$-2-Br-*arachno*-$B_{10}H_{11}$ **3a**, *exo*-6,*endo*-9-$(PMe_2Ph)_2$-2-Br-*arachno*-$B_{10}H_{11}$ **3b** and *endo*-6,*exo*-9-$(PMe_2Ph)_2$-2-Br-*arachno*-$B_{10}H_{11}$ **3c**[a]

	3a[b]		**3b**[c]		**3c**[d]	
Position	$\delta(^{11}B)$	$\delta(^{1}H)$	$\delta(^{11}B)$	$\delta(^{1}H)$	$\delta(^{11}B)$	$\delta(^{1}H)$
2	+1.0	—	+3.9	—	+9.8	—
4	−4.0	+2.15	+6.7	+2.95[e]	+0.6	+2.25
1,3	−36.5	+1.00	−32.2	+1.28	−32.1	+1.27
6	−33.6[f]	−1.05	−33.1[g]	−1.53	−27.7[h]	+1.65
9	*ca.* −36[i]	−1.04	−31.0[g]	+0.99	−35.6[f]	−1.50
5,7	−17.9	+2.06	−13.9	+2.16	−13.7	+1.85
8,10	−19.6	+1.63	−19.0	+1.65	−17.6	+1.95

[a] In $CDCl_3$ at 294 K; $\delta(^{1}H)$ related to directly bound B positions by ^{1}H-{^{11}B(selective)} spectroscopy; any fine structure noted for ^{1}H resonances is observed under conditions of complete {^{11}B(broad-band noise)} decoupling. [b] $\delta(^{31}P)$ *ca.* −2 (br); additionally $\delta(^{1}H)$[μ-H(5,10 and 7,8)] −4.16, $\delta(^{1}H)(PMe_2)$ +1.88 with $^{2}J(^{31}P–^{1}H)$ = 11.5 Hz and $\delta(^{1}H)$(PPh) +7.50 to +7.73. [c] $\delta(^{31}P)$ *ca.* +11 and −2 (both broad); additionally $\delta(^{1}H)$[μ-H(5,10 and 7,8)] −4.96 with $^{2}J(^{31}P–^{1}H)$ *ca.* 10, $\delta(^{1}H)(PMe_2)$ +1.77 with $^{2}J(^{31}P–^{1}H)$ = 11.8 and +1.63 with $^{2}J(^{31}P–^{1}H)$ = 13.0 Hz and $\delta(^{1}H)$(PPh) +7.29 to +7.73. [d] $\delta(^{31}P)$ *ca.* +9 and 0 (both broad); additionally $\delta(^{1}H)$[μ-H(5,10 and 7,8)] −4.83 with $^{2}J(^{31}P–^{1}H)$ *ca.* 14, $\delta(^{1}H)(PMe_2)$ +1.83 with $^{2}J(^{31}P–^{1}H)$ = 11.5, and +1.44 with $^{2}J(^{31}P–^{1}H)$ = 11.5 Hz and $\delta(^{1}H)$(PPh) +7.30 to +7.73. [e] Coupling $^{3}J(^{31}P–^{1}H)$ *ca.* 23 Hz. [f] Coupling $^{1}J(^{31}P–^{11}B)$ *ca.* 130 Hz. [g] Coupling $^{1}J(^{31}P–^{11}B)$ *ca.* 130 Hz; not measurable more accurately due to overlap with ^{11}B(1,3). [h] Coupling $^{1}J(^{31}P–^{11}B)$ *ca.* 125 Hz. [i] Not measurable more accurately due to overlap with ^{11}B(1,3).

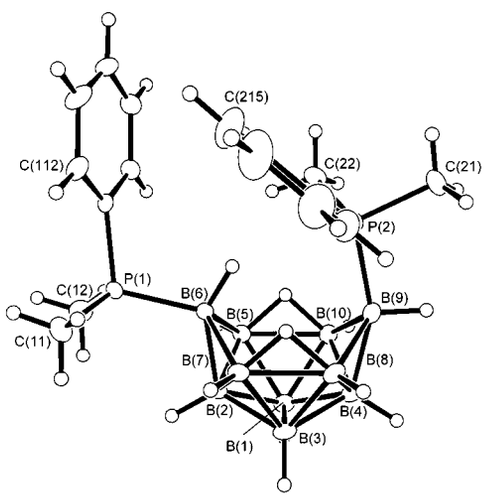

Fig. 2 An ORTEP-type[10] drawing of the crystallographically determined molecular structure of *exo*,*endo*-6,9-$(PMe_2Ph)_2$-*arachno*-$B_{10}H_{12}$ **1b** drawn with the same conventions as in Fig. 1

III

In the *exo*,*endo* compound **1b** significant structural effects attributable to the *endo* ligand appear to be localized around its point of attachment, and there appears to be a systematic weakening of the bonding around the *endo*-substituted boron atom B(9). Thus the boron–phosphorus distance B(9)–P(2)(*endo*) in **1b** is 1.941(2) Å, significantly longer than the B(6)–P(*exo*) and B(9)–P(*exo*) distances in **1a** and **1b** [range 1.912(3)–1.925(3) Å]. The three interboron connectivities adjacent to this B(9)–P(2)(*endo*) linkage in compound **1b** are also elongated relative to the corresponding separations in the '*exo*' cluster fragments of **1a** and **1b**. Specifically, B(4)–B(9) is 1.762(2) Å in **1b** compared to a range of 1.732(4)–1.748(4) Å for the other B(2)–B(6) and B(4)–B(9) distances in **1a** and **1b**, and B(8)–B(9) and B(9)–B(10) are 1.888(2) and 1.883(2) Å respectively in **1b** compared to a range of 1.851(2)–1.877(4) Å for the other B(8)–B(9), B(9)–B(10), B(5)–B(6) and B(6)–B(7) distances in **1a** and **1b**. Moreover, there is a small but significant enlargement [2.5(2) to 4.2(2)°] of the B(7)–B(8)–B(9) and B(9)–B(10)–B(5), angles, and similarly [1.4(2) to 3.2(2)°] of the B(1)–B(4)–B(9) and B(3)–B(4)–B(9) angles, at the *endo*-substituent end of compound **1b** relative to the equivalent parameters in the *exo*-configured fragments of **1a** and **1b**. All of these structural effects could be perhaps be attributable to the minimization of steric factors arising from organic groups associated with the *endo*-phosphine substituent in isomer **1b**. However, there must be an underlying electronic contribution to these features, as these deviations appear to be limited strictly to the *endo* end of the cluster in the *exo*,*endo* isomer **1b**. The relative weakness of these linkages to the *endo*-substituted boron atoms are further manifested in the relatively facile thermal isomerization of *endo*,*exo* **1b** to generate the *exo*,*exo* isomer **1a** of greater thermodynamic stability.

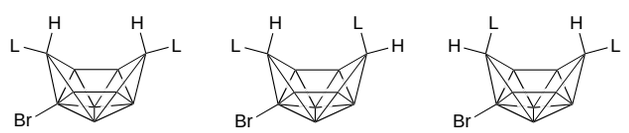

Having unequivocally confirmed the *exo*,*endo* structural type, it was of interest to examine the reaction of the halogenated derivative 2-Br-*nido*-$B_{10}H_{13}$ with PMe_2Ph under the same conditions for any differential influence that the 2-bromo substituent might have in dictating a 6,9 (structure **V**) *versus* a 9,6 (structure **VI**) *exo*,*endo* configuration on the *nido*/*arachno* 2-bromodecaboranyl matrix. Additionally, it would yield confirmation of the retention of the 2-bromo configuration in the conversion from ten-vertex *nido* into ten-vertex *arachno* in this type of reaction. Although this last was established some time ago for $L = SMe_2$ by NMR spectroscopy,[12] the earlier experiment was necessarily conducted at the lower dispersions available at the time, and so we thought it of interest to examine for product purity and isomeric purity by NMR spectroscopy at the higher dispersions now available.

In the event, addition of PMe_2Ph to 2-Br-*nido*-$B_{10}H_{13}$ at *ca.* 200 K resulted in clean formation of two products, **3b** and **3c**, in equimolar ratio within experimental error by integrated ^{11}B NMR spectroscopy. These were isolated by TLC and identified and distinguished by ^{1}H and ^{11}B NMR spectroscopy (Table 3) as the 6,9-*exo*,*endo* and 9,6-*exo*,*endo* isomers of 6,9-(PMe_2Ph)-2-Br-*arachno*-$B_{10}H_{11}$ (compounds **3b** and **3c** respectively). The differential NMR assignment was confirmed by single-crystal X-ray diffraction work on the 6,9-*exo*,*endo* isomer **3b**. No other significant products were detectable. In particular the conventionally structured 6,9-*exo*,*exo* isomer **3a** (schematic **IV**) was absent, indicating that an effect of the 2-bromo substituent is to divert all of the kinetic product into an *exo*,*endo* configuration. This tendency was confirmed by the examination of the

Table 4 Measured ^{11}B and ^{1}H NMR data for *exo*,*endo*-6,9-$(PMe_2Ph)_2$-2,4-Cl_2-*arachno*-$B_{10}H_{10}$ **4b**[a]

Assignment	δ(^{11}B)	δ(^{1}H)[b]
2 or 4	+15.1	—
2 or 4	+8.8	—
1,3	−30.9	+1.49
6	−35.4[c]	−1.44
9	*ca.* −30[d]	+1.45
5,7	−14.4	+2.10
8,10	−19.0	+1.82

[a] In $CDCl_3$ at 294 K; additionally δ(^{31}P) *ca.* +10 and −1 (both broad); δ(^{1}H) related to directly bound B positions by ^{1}H-{^{11}B(selective)} spectroscopy; any fine structure noted for the ^{1}H resonances is observed under conditions of complete {^{11}B(broad-band noise)} decoupling. [b] Additionally δ(^{1}H)[μ-H(5,10 and 7,8)] −4.73 with $^{2}J(^{31}P–^{1}H)$ *ca.* 12, δ(^{1}H)(PMe_2) +1.70 with $^{2}J(^{31}P–^{1}H)$ = 11.5 Hz and δ(^{1}H)(PPh) +7.21 to +7.70. [c] $^{1}J(^{31}P–^{11}B)$ *ca.* 125 Hz. [d] Not measurable more accurately due to overlap with ^{11}B(1,3).

Table 5 Selected interatomic distances (Å) and angles (°) for *exo*-6,*endo*-9-$(PMe_2Ph)_2$-2-Br-*arachno*-$B_{10}H_{11}$ **3**

Br(2)–B(2)	1.986(4)	B(3)–B(7)	1.790(6)
P(1)–B(6)	1.914(4)	B(3)–B(8)	1.796(6)
B(1)–B(4)	1.742(6)	B(4)–B(10)	1.759(6)
B(1)–B(2)	1.754(6)	B(4)–B(9)	1.759(6)
B(1)–B(5)	1.773(6)	B(4)–B(8)	1.759(6)
B(1)–B(10)	1.780(6)	B(5)–B(6)	1.879(6)
B(1)–B(3)	1.822(6)	B(5)–B(10)	1.887(6)
B(2)–B(6)	1.717(6)	B(6)–B(7)	1.846(5)
B(2)–B(5)	1.747(6)	B(7)–B(8)	1.906(6)
B(2)–B(3)	1.755(6)	B(8)–B(9)	1.869(6)
B(2)–B(7)	1.766(5)	B(9)–B(10)	1.882(6)
B(3)–B(4)	1.744(7)		
B(6)–B(2)–B(1)	117.9(3)	B(2)–B(6)–P(1)	118.1(3)
B(6)–B(2)–B(3)	117.0(3)	B(5)–B(6)–P(1)	121.8(2)
B(1)–B(2)–Br(2)	116.5(3)	B(7)–B(6)–P(1)	122.1(3)
B(3)–B(2)–Br(2)	117.2(3)	B(6)–B(7)–B(8)	113.9(3)
B(5)–B(2)–Br(2)	118.8(2)	B(9)–B(8)–B(7)	117.4(3)
B(6)–B(2)–Br(2)	115.5(3)	B(8)–B(9)–B(10)	101.8(3)
B(7)–B(2)–Br(2)	120.0(3)	B(4)–B(9)–P(2)	158.0(3)
B(1)–B(4)–B(9)	118.7(3)	B(8)–B(9)–P(2)	111.1(2)
B(3)–B(4)–B(9)	118.6(3)	B(10)–B(9)–P(2)	112.2(2)
B(6)–B(5)–B(10)	113.8(3)	B(9)–B(10)–B(5)	117.5(3)
B(7)–B(6)–B(5)	104.5(3)		

Cluster B–B–B acute angles are within the range 56.4(2)–64.7(2)°.

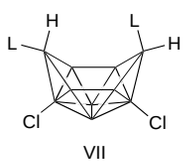

VII

same reaction using 2,4-Cl_2-*nido*-$B_{10}H_{12}$ as starting substrate. At *ca.* 200 K with PMe_2Ph this gave a quantitative conversion into *exo*,*endo*-6,9-$(PMe_2Ph)_2$-2,4-Cl_2-*arachno*-$B_{10}H_{10}$ (compound **4b**, schematic structure **VII**). Thus there was no evidence for the symmetrical *exo*,*exo* isomer **4a**, nor for any significant quantities of {$B_{10}H_{10}Cl_2$} residues other than the 2,4-dichloro configuration. That reaction (1) proceeds without a rearrangement of the {B_{10}} skeleton tends therefore to be confirmed. The NMR data for *exo*,*endo*-6,9-$(PMe_2Ph)_2$-2,4-Cl_2-*arachno*-$B_{10}H_{10}$ (**4b**) are in Table 4.

As mentioned in the previous paragraph, the 6-*exo*,9-*endo* isomer of the 2-brominated species, compound **3b**, has been examined by a single-crystal X-ray diffraction analysis (Fig. 3 and Table 5), which unequivocally establishes this isomer to be of structure type **V** and confirms our analysis of the NMR spectra of **3b** and, by implication, **3c**. The hydrogen-bridged connectivities B(5)–B(10) and B(7)–B(8) [1.887(6) and 1.906(6) Å respectively] are comparable to those in **1a** and **1b** and again confirm the *arachno* character of the cluster. Cluster flexing around the B(9) atom of the kind seen in **1b**, which we have associated with the presence of an *endo versus* an *exo* phosphine substituent, is also observed in compound **3b**. Specifically, (*a*) the B(9)–P(*endo*) distance of 1.928(4) Å in **3b** is towards the long end of the range established above for B(6)–P(*exo*) and B(9)–P(*exo*) distances [1.912(3)–1.925(3) Å], (*b*) the interboron distance B(4)–B(9) of 1.759(6) Å is much longer than the range of equivalent distances in the *exo*-substituted fragments of **1a** and **1b** [1.732(4)–1.748(4) Å], and (*c*) there are even greater increases in the B(7)–B(8)–B(9), B(9)–B(10)–B(5), B(1)–B(4)–B(9) and B(3)–B(4)–B(9) angles in **3b** compared to the equivalent values for the *exo*-substituted fragments of **1a** and **1b**. It may also be expected that the bromo substituent on the B(2) position would also have some differential structural influences, and could contribute to variation of all the geometric parameters determined for **3b** compared to those of unsubstituted **1a** and **1b**. In accord with this, for example, all of the interboron distances involving B(2) are rather shorter than the equivalent separations in **1a** and **1b**; in particular B(2)–B(6) is only 1.717(6) Å, short for such a connectivity.

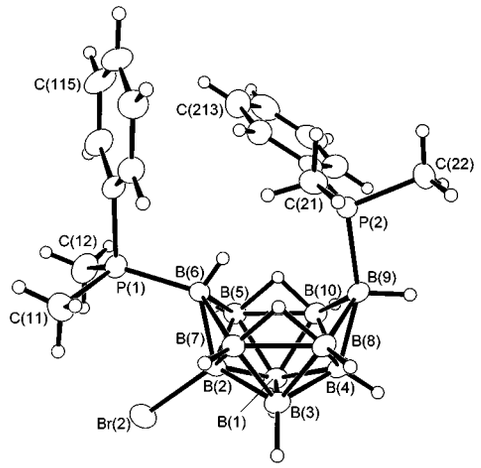

Fig. 3 An ORTEP-type[10] drawing of the crystallographically determined molecular structure of *exo*-6,*endo*-9-$(PMe_2Ph)_2$-2-Br-*arachno*-$B_{10}H_{11}$ **3b** drawn with the same conventions as in Fig. 1

It was previously reported that *exo*,*endo*-6,9-$(PMe_2Ph)_2$-*arachno*-$B_{10}H_{12}$ **1b** converts quantitatively into its *exo*,*exo* isomer **1a** on heating in $CD_3C_6D_5$ solution.[8] More exact work now shows that the reaction occurs with half-life $t_{\frac{1}{2}}$ *ca.* 30 min in *ca.* 0.05 M $CD_3C_6D_5$ solution at 343 K. The 2-Br derivatives are marginally less labile, with $t_{\frac{1}{2}}$ *ca.* 45 min at 343 K for the *exo*,*endo* ⟶ *exo*,*exo* conversion under the same conditions. By contrast, the dichloro species *exo*,*endo*-6,9-$(PMe_2Ph)_2$-2,4-Cl_2-*arachno*-$B_{10}H_{10}$ (compound **4b**) seems much more stable, with no sign of change on heating at 343 K over similar periods to those that effect the quantitative isomerization of the monobromo compounds **3b** and **3c**. More extended heating appears to result in a more general decomposition. It may be noted that without rigorous exclusion of moisture these thermolyses result in boron-vertex loss to generate 4-(PMe_2Ph)-*arachno*-B_9H_{13}. As with the initial *exo*,*endo* synthesis, the *exo*,*endo* ⟶ *exo*,*exo* conversions are quantitative and isomerically pure, suggesting no irreversible cluster-framework rearrangement during the conversion. The 6,9-L_2-*arachno*-$B_{10}H_{12}$ system is quite robust when L is a ligand such as phosphine, so a dissociative mechanism for the *exo*,*endo* ⟶ *exo*,*exo* conversion is perhaps unlikely. Extrusion of the {$BH(PMe_2Ph)$} vertex, rotation, and reincorporation is therefore a possibility. Here it may be pertinent that substantiated phosphine-induced vertex-extrusion mechanisms are recently precedented in boron-containing cluster chemistry.[13]

The NMR data for the *exo*,*exo* form of 6,9-$(PMe_2Ph)_2$-2-Br-

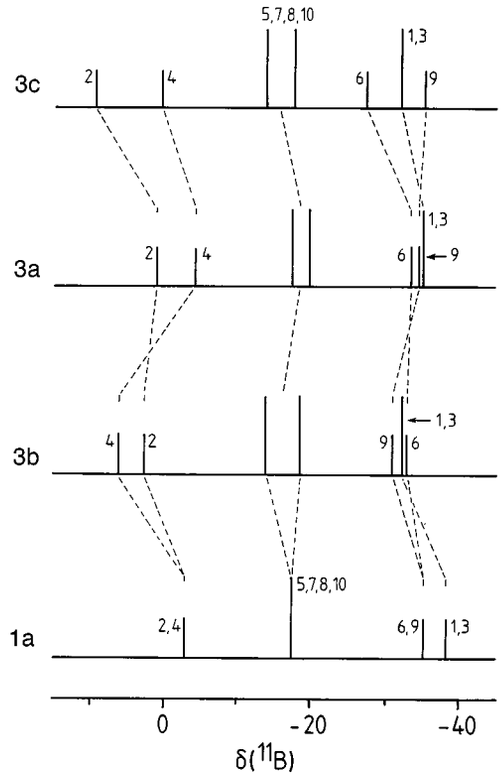

Fig. 4 Stick diagrams of the relative intensities and chemical shifts in the ^{11}B NMR spectra of (from bottom to top) *exo*,*exo*-6,9-$(PMe_2Ph)_2$-*arachno*-$B_{10}H_{12}$ **1a**, *exo*-6,*endo*-9-$(PMe_2Ph)_2$-2-Br-*arachno*-$B_{10}H_{11}$ **3b**, *exo*,*exo*-6,9-$(PMe_2Ph)_2$-2-Br-*arachno*-$B_{10}H_{11}$ **3a** and *endo*-6,*exo*-9-$(PMe_2Ph)_2$-2-Br-*arachno*-$B_{10}H_{11}$ **3c**. Hatched lines join selected equivalent positions among the four species

arachno-$B_{10}H_{11}$ **3a** are given in Table 3 along with corresponding data for its *endo*,*exo* isomers **3b** and **3c**; NMR data for *exo*,*endo*-6,9-$(PMe_2Ph)_2$-2,4-Cl_2-*arachno*-$B_{10}H_{10}$ **4b** are given in Table 4. The ^{11}B spectra of the three 2-Br isomers **3a**–**3c** are compared graphically with the spectrum[8] of unsubstituted *exo*,*exo*-6,9-$(PMe_2Ph)_2$-*arachno*-$B_{10}H_{12}$ **1a** in Fig. 4. Compared to its unsubstituted parent **1a** there is a downfield shift of *ca.* 4 ppm for the bromine-substituted 2 position in **3a**. This is within established ranges.[12,14] For the two *exo*,*endo* compounds **3b** and **3c** the resonances of the boron atoms B(2) and B(4) are shifted to low field relative to those of the *exo*,*exo* compound **3a**. The magnitude of the downfield shift is 10.7 and 8.8 ppm for the boron atoms adjacent to the site of *endo* substitution [respectively B(4) in **3b** and B(2) in **3c**], and 2.9 and 3.6 ppm for those adjacent to the site of *exo* substitution [respectively B(2) in **3b** and B(4) in **3c**]. Similarly, atoms B(6) and B(9) bound to phosphorus are deshielded in **3b** and **3c** compared to **3a**. If the phosphine is in the *endo* position this shift of the resonances to higher frequency is greater [4.0 ppm for B(9) in **3b** and 5.9 ppm for B(6) in **3c**] than if the phosphine is in the *exo* position [essentially unchanged at 0.5 ppm for B(6) in **3b** and 0.6 ppm for B(9) in **3c**]. A similar pattern of the chemical shifts would presumably occur in the dichlorodecaborane system, but in the absence of *exo*-*exo*-6-9-$(PMe_2Ph)_2$-2,4-Cl_2-*arachno*-$B_{10}H_{10}$ **4a** we are unable to confirm this.

The ^1H NMR properties of the {BH(PMe_2Ph)} groupings at the 6 and 9 positions merit comment since these are instrumental in distinguishing the stereochemistry of the mixed species of the types **3a**–**3c** in the absence of diffraction results. Comparison of the *exo*,*endo* forms of the parent species 6,9-$(PMe_2Ph)_2$-*arachno*-$B_{10}H_{12}$ **1b** with its symmetrical *exo*,*exo* analogue **1a** readily shows that the {BH(*exo*)} unit of the *endo*-phosphinated 6 or 9 position resonates at $\delta(^1H) + 1.01$, whereas the {BH(*endo*)} unit of an *exo*-phosphinated 6 or 9 position resonates at $\delta(^1H) - 1.41$. This differential behaviour is in accord with the general shielding behaviour of *endo versus exo* {BH} protons.[14] This behaviour, allied with the results of ^1H-{^{11}B} correlation work, and of [^1H–^1H] and [^{11}B–^{11}B] correlation spectroscopy (COSY), is consistent with the assignment of the spectra and the consequent NMR substantiation of the three isomers **3a**–**3c** in the 6,9-$(PMe_2Ph)_2$-2-Br-*arachno*-$B_{10}H_{11}$ system (Table 3).

Experimental

General

Reactions were carried out in dry solvents under dry nitrogen but subsequent manipulatory and separatory procedures were carried out in air. Preparative thin-layer chromatography (TLC) was carried out using 1.00 mm layers of silica gel G (Merck, type GF_{254}) made from water slurries on glass plates of dimensions 20 × 20 cm^2, followed by drying in air at 80 °C. The compound PMe_2Ph was obtained commercially, and 2-$BrB_{10}H_{13}$ and 2,4-$Cl_2B_{10}H_{12}$ were prepared essentially as reported elsewhere.[15]

Nuclear magnetic resonance spectroscopy

NMR spectroscopy was performed at *ca.* 5.9 and 9.4 T (fields corresponding to 250 and 400 MHz ^1H frequencies respectively) using commercially available instrumentation and using techniques and procedures described and enunciated elsewhere.[8,16–18] Chemical shifts δ are given in ppm relative to Ξ = 100 MHz for $\delta(^1H)$ (± 0.05 ppm) (nominally $SiMe_4$), 32.083 972 MHz for $\delta(^{11}B)$ (±0.5 ppm) (nominally $Et_2O{\cdot}BF_3$ in $CDCl_3$),[14] and 40.480 730 MHz for $\delta(^{31}P)$ (± 0.05 ppm) (nominally 85% aqueous H_3PO_4); Ξ is as defined in ref. 19.

Preparations

***exo*,*exo*-6,9-$(PMe_2Ph)_2$-*arachno*-$B_{10}H_{12}$ 1a and *exo*,*endo*-6,9-$(PMe_2Ph)_2$-*arachno*-$B_{10}H_{12}$ 1b.** A sample of $B_{10}H_{14}$ (100 mg, 0.82 mmol) was dissolved in tetrahydrofuran (thf) (20 cm^3), cooled to *ca.* 200 K, and then PMe_2Ph (226 mg, 233 μl, 1.64 mmol) was added. The solution was stirred for 15 min at low temperature, then at room temperature for 2 h. The more volatile components were removed, the solid residue was redissolved in CH_2Cl_2 (*ca.* 5 cm^3) and the products were separated and purified by repeated preparative TLC, ultimate development with hexane–CH_2Cl_2 (10 : 90) giving two products. These were *exo*,*exo*-6,9-$(PMe_2Ph)_2B_{10}H_{12}$ **1a** (185 mg, 0.47 mmol, 57%; R_f 0.85) and *exo*,*endo*-6,9-$(PMe_2Ph)_2B_{10}H_{12}$ **1b** (120 mg, 0.28 mmol, 34%; R_f 0.70).

***exo*-6,*endo*-9-$(PMe_2Ph)_2$-2-Br-*arachno*-$B_{10}H_{11}$ 3b and *endo*-6,*exo*-9-$(PMe_2Ph)_2$-2-Br-*arachno*-$B_{10}H_{11}$ 3c.** A sample of 2-$BrB_{10}H_{13}$ (51 mg, 250 μmol) was dissolved in CH_2Cl_2 (20 cm^3) at *ca.* 200 K, and then PMe_2Ph (70 mg, 72 μl, 500 μmol) was added. The solution was stirred for 15 min at low temperature, allowed to warm to room temperature, and then stirred for 2 h. The more volatile components were removed, the solid residue was redissolved in 100% CH_2Cl_2 (*ca.* 5 cm^3) and the products were separated and purified by repeated preparative TLC, development with CH_2Cl_2 giving two products. These were *exo*-6,*endo*-9-$(PMe_2Ph)_2$-2-Br-*arachno*-$B_{10}H_{11}$ **3b** (54 mg, 114 μmol, 45%; R_f 0.70) and *endo*-6,*exo*-9-$(PMe_2Ph)_2$-2-Br-*arachno*-$B_{10}H_{11}$ **3c** (52 mg, 110 μmol, 43%; R_f 0.56).

***exo*-6,*endo*-9-$(PMe_2Ph)_2$-2,4-Cl_2-*arachno*-$B_{10}H_{10}$ 4b.** A sample of 2,4-Cl_2-*nido*-$B_{10}H_{12}$ (36 mg, 190 μmol) was dissolved in CH_2Cl_2 (10 cm^3), and then PMe_2Ph (52 mg, 54 μl, 380 μmol) was added at *ca.* 200 K. The solution was stirred for 15 min at low temperature, allowed to warm to room temperature, and then stirred at room temperature for 2 h. Monitoring by ^{11}B NMR spectroscopy showed a quantitative conversion into the

Table 6 Crystallographic data and details of data collection and structure refinement for compounds **1a**, **1b** and **3b**

	1a[a]	**1b**	**3b**
Formula	$C_{16}H_{34}B_{10}P_2$	$C_{16}H_{34}B_{10}P_2$	$C_{16}H_{33}B_{10}BrP_2$
M_r	396.47	396.47	475.37
Crystal dimensions/mm	0.89 × 0.54 × 0.12	0.79 × 0.67 × 0.53	0.54 × 0.49 × 0.42
Crystal appearance	Colourless rod	Colourless block	Colourless block
Crystal system	Monoclinic	Triclinic	Monoclinic
Space group	$P2_1$	$P\bar{1}$	$P2_1/n$
a/Å	13.4155(9)	8.6670(4)	14.3789(12)
b/Å	12.0113(7)	10.3130(6)	11.8018(7)
c/Å	16.0081(12)	14.5912(9)	16.4193(12)
α/°	—	102.741(5)	—
β/°	113.704(6)	101.783(5)	114.418(7)
γ/°	—	103.293(5)	—
U/Å^3	2361.9(3)	1192.53(12)	2537.1(3)
Z	4	2	4
F(000)	840	420	976
D_c/Mg m^{-3}	1.115	1.104	1.245
μ/mm^{-1}	1.632	0.183	3.379
$\theta_{orientation}$/°	30.1–34.9	15.5–17.5	33.1–41.7
$\theta_{data\ collection}$/°	3.01–64.34	2.11–24.97	3.45–64.41
h,k,l ranges	−15 to 15, −13 to 11, −18 to 18	−10 to 10, −12 to 12, −17 to 17	−16 to 16, −13 to 13, −19 to 19
Data measured	7803	8380	5308
Unique data, n	7227	4190	3892
Crystal decay (%)	9.2	0	3.7
R_{int}[b]	0.0227	0.0199	0.0455
T_{min}, T_{max}	0.723, 0.862	—	0.181, 0.358
Observed data [$F_o > 2\sigma(I)$]	6962	3998	3779
$R1$,[c] $wR2$[d] (observed data)	0.0388, 0.1012	0.0302, 0.0829	0.0546, 0.1587
(all data)	0.0416, 0.1100	0.0333, 0.0888	0.0555, 0.1604
Goodness of fit on F^2, S[e]	1.062	1.002	1.150
Weighting parameters, g_1, g_2[f]	0.0665, 0.9854	0.0457, 0.5289	0.0923, 4.1653
Number of parameters, p	609	305	310
Largest difference peak and hole/e Å^{-3}	0.27, −0.39	0.26, −0.32	0.80, −1.16

[a] Flack absolute structure parameter[20] 0.01(2). [b] $R_{int} = \Sigma|F_o^2 - F_o^2(\text{mean})|/\Sigma F_o^2$. [c] $R1 = \Sigma||F_o| - |F_c||/\Sigma|F_o|$. [d] $wR2 = [\Sigma w(F_o^2 - F_c^2)^2/\Sigma(F_o^2)^2]^{\frac{1}{2}}$. [e] $S = [\Sigma w(F_o^2 - F_c^2)^2/(n-p)]^{\frac{1}{2}}$. [f] Weighting scheme $w^{-1} = [\sigma^2(F_o^2) + (g_1P)^2 + g_2P]$ where $P = (F_o^2 + 2F_c^2)/3$.

species isolated and identified as compound **4b**. The more volatile components were removed, the solid residue was redissolved in CH_2Cl_2 (*ca.* 5 cm^3) and subjected to preparative TLC, development with CH_2Cl_2 giving one product only. This was *exo*-6,*endo*-9-$(PMe_2Ph)_2$-2,4-Cl_2-*arachno*-$B_{10}H_{10}$ **4b** (81 mg, 174 μmol, 93%; R_f 0.75).

Crystallography

Crystals of compounds **1a**, **1b** and **3b** suitable for single-crystal X-ray diffraction analysis were each grown from CH_2Cl_2–hexane at room temperature. All crystallographic measurements were carried out at 160(2) K on a Stoe STADI 4 four-circle diffractometer operating in the ω–θ scan mode using graphite-monochromated X-radiation (Cu-Kα, $\bar{\lambda}$ = 1.541 86 Å for **1a** and **3b**; Mo-Kα, $\bar{\lambda}$ = 0.710 73 Å for **1b**). Crystal data and refinement parameters for the three crystals are listed in Table 6. Cell dimensions were refined from the values of 50 (for **1a**), 70 (for **1b**) or 30 (for **3b**) selected reflections (together with their Friedel opposites) that were well separated in reciprocal space and that were measured at ± θ in order to minimize systematic errors. The three sets of data were corrected for Lorentz and polarization effects. An empirical absorption correction based on ψ scans was applied to the data sets collected for compounds **1a** and **3b**. The structures of the three compounds were solved by direct methods using SHELXS 86[21] and were refined by full-matrix least squares (against all the unique F^2 data) using SHELXL 93.[22] Refinement was similar for all three structures. Two independent molecules of compound **1a** are present in the asymmetric unit. All non-hydrogen atoms were refined with anisotropic displacement parameters. Phosphine hydrogen atoms were constrained to idealized positions with a riding model that included free rotation of methyl groups and with PPh units restrained to be flat and of overall C_{2v} symmetry. Cluster hydrogen atoms were located *via* Fourier-difference syntheses and freely refined with isotropic displacement parameters. The crystallographically imposed absolute structure of the crystal of compound **1a** was confirmed by the refinement of the Flack absolute structure parameter[20] to 0.01(2).

CCDC reference number 186/764.

Acknowledgements

We thank the Deutsche Forschungsgemeinschaft, and the UK EPSRC (grant nos. GR/F/78323, GR/J/56929 and GR/K/05818) for support.

References

1 R. Schaeffer, *J. Am. Chem. Soc.*, 1957, **79**, 1006.
2 S. G. Shore in *Boron Hydride Chemistry*, ed. E. L. Muetterties, Academic Press, New York, 1975, pp. 144–146 and refs. therein.
3 T. L. Heying, J. W. Ager, jun., S. L. Clark, D. J. Mangold, H. L. Goldstein, M. Hillman, R. J. Polak and J. W. Szymanski, *Inorg. Chem.*, 1963, **2**, 1089; M. M. Fein, D. Grafstein, J. E. Paustan, J. Bobinski, B. M. Lichstein, N. Mayes, N. Schwartz and M. S. Cohen, *Inorg. Chem.*, 1963, **2**, 1115; M. M. Fein, J. Bobinski, N. Mayes, N. Schwartz and M. S. Cohen, *Inorg. Chem.*, 1963, **2**, 1111; M. F. Hawthorne, T. D. Andrews, P. M. Garrett, F. P. Olsen, M. Reintjes, F. N. Tebbe, L. F. Warren, P. A. Wegner and D. C. Young, *Inorg. Synth.*, 1968, **10**, 91; W. Clegg, R. Coult, M. A. Fox, W. R. Gill, J. A. H. MacBride and K. Wade, *Polyhedron*, 1993, **12**, 2711; W. E. Hill, F. A. Johnson and R. W. Novak, *Inorg. Chem.*, 1975, **14**, 1244; S. Islam, F. A. Johnson, W. E. Hill and L. M. Silva-Trivino, *Inorg. Chim. Acta*, 1997, **260**, 99.
4 J. Reddy and W. N. Lipscomb, *J. Am. Chem. Soc.*, 1959, **81**, 754; *J. Chem. Phys.*, 1959, **31**, 610.
5 D. E. Sands and A. Zalkin, *Acta Crystallogr.*, 1962, **15**, 410.
6 T. M. Polyanskaya and V. V. Volkov, *Zh. Strukt. Khim*, 1989, **30**, 116.

7 T. Polyanskaya, *Abstracts Ninth International Meeting on Boron Chemistry*, *Heidelberg*, *Germany*, 14–18 July, 1996, Abstract no. P117, p. 210.
8 X. L. R. Fontaine and J. D. Kennedy, *J. Chem. Soc.*, *Dalton Trans.*, 1987, 1573.
9 S. M. Cendrowski-Guillaume, J. L. O'Loughlin, I. Pelczer and J. T. Spencer, *Inorg. Chem.*, 1995, **34**, 3935.
10 ORTEX, version 5, P. McArdle, *J. Appl. Crystallogr.*, 1995, **28**, 65.
11 M. Thornton-Pett, M. A. Beckett and J. D. Kennedy, *J. Chem. Soc.*, *Dalton Trans.*, 1986, 303.
12 T. L. Heying and C. Naar-Colin, *Inorg. Chem*, 1964, **3**, 282.
13 L. Barton, J. Bould, H. Fang, K. Hupp, N. P. Rath and C. Gloeckner, *J. Am. Chem. Soc.*, 1997, **119**, 631 and refs. therein.
14 See, for example, J. D. Kennedy in *Multinuclear NMR*, ed. J. Mason, Plenum, New York and London, 1987, ch. 8, pp. 221–254 and refs. therein.
15 R. F. Sprecher, B. E. Aufderheide, G. W. Luther III and J. C. Carter, *J. Am. Chem. Soc.*, 1974, **96**, 4404.
16 See, for example, M. A. Beckett, M. Bown, X. L. R. Fontaine, N. N. Greenwood, J. D. Kennedy and M. Thornton-Pett, *J. Chem. Soc.*, *Dalton Trans.*, 1988, 1969 and refs. therein.
17 See, for example, G. Ferguson, J. D. Kennedy, X. L. R. Fontaine, Faridoon and T. R. Spalding, *J. Chem. Soc.*, *Dalton Trans.*, 1988, 2555 and refs. therein.
18 See, for example, D. Reed, *Chem. Soc. Rev.*, 1993, **22**, 109 and refs. therein.
19 W. McFarlane, *Proc. R. Soc. London*, *Ser. A*, 1968, **306**, 185.
20 H. D. Flack, *Acta Crystallogr.*, *Sect. A*, 1983, **39**, 876.
21 G. M. Sheldrick, SHELXS 86, Program for crystal structure solution, University of Göttingen, 1986.
22 G. M. Sheldrick, SHELXL 93, Program for crystal structure refinement, University of Göttingen, 1993.

Received 5*th August* 1997; *Paper* 7/05696F